RSC Advances

ROYAL SOCIETY OF CHEMISTRY

www.rsc.org/advances

Table of Content

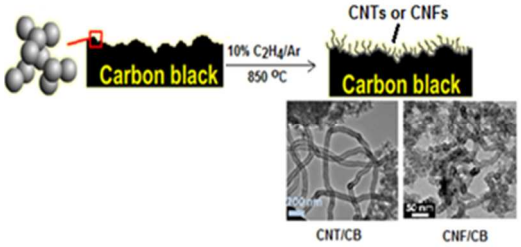

Carbon black can act as catalysts to grow carbon nanotubes or carbon nanofibers through a metal-free thermal chemical deposition.

Cite this: DOI: 10.1039/c0xx00000x

www.rsc.org/xxxxxx

PAPER

Metal-Catalyst-Free Growth of Carbon Nanotubes/Carbon Nanofibers on Carbon Blacks Using Chemical Vapor Deposition

Zhi-Yan Zeng and Jarrn-Horng Lin*

Received (in XXX, XXX) Xth XXXXXXXXX 20XX, Accepted Xth XXXXXXXXX 20XX

DOI: 10.1039/b000000x

Metal-catalyst-free growth of carbon nanostructures, e.g. carbon nanotubes (CNTs) or carbon nanofibers (CNFs), on typical materials is a promising route to achieve further applications without interference of unwanted metal catalysts. Here, we report that carbon black (CB) can act as catalysts to controllably grow CNTs or CNFs yielding a bi-functional hybrid structure-CNTs/CB or CNFs/CB through a metal-catalyst-free chemical vapour deposition (MCF-CVD) in a reaction temperature range of 800-950 °C. We find that the decomposition steps of carbon source is a crucial factor to determine the formation of CNTs (ethylene), CNFs (acetylene) or amorphous carbons (ethanol and cyclohexane) evidenced by the gas-composition analysis. The growth yields of CNTs or CNFs catalysed by various CBs display a linear corresponding with the surface areas of CBs, indicating that structural morphologies of CB dominate the growth of carbon nanostructures. The formation of CNTs/CB or CNFs/CB is proposed to obey the vapour-solid-surface-solid model with an activation energy of 59.0 kJ/mol. The growth mechanism of CNTs/CB or CNFs/CB is suggested that a direct dehydrogenation route of carbon sources (ethylene and acetylene) would occur on CB surfaces through self-assembling. The multi-step decomposition route of carbon sources (ethanol and cyclohexane) would generate amorphous carbons only. These findings open a new route to prepare unique carbon structures through a metal-catalyst-free CVD.

Introduction

The unique physicochemical properties of carbon nanotubes (CNTs) have led to the rapid development of CNT synthetic techniques during the past two decades. However, two main issues impact the applications of pristine CNTs: (1) residual metal-catalyst particles remain within CNTs and (2) difficulty in dispersing pristine CNTs well in aqueous or polymer matrices. Accordingly, several reports have demonstrated post-treated techniques to generate high-purity CNTs and to give a well-dispersion of CNTs in polymers.[1-4] Nevertheless, the post-treatments of CNTs will be complex and not benefit for a low-cost production. A potential solution for the above problems is to grow CNTs on desired substrates or matrices through a metal-catalyst-free route. Recently, several reports have demonstrated the pathways for growing CNTs on SiO_2,[5-7] nano-diamond[8] and defect-rich carbon surfaces[9, 10] without the assistance of metal catalysts. These methods open up new routes for the synthesis of CNTs without metal catalysts, though the growth mechanisms in the above studies and their potential applications need more studies.

Here, we systematically study a simple process to directly grow CNTs over carbon black (CB) using metal-catalyst-free chemical vapour deposition (MCF-CVD) without the assistance of metal catalyst particles. Previouly, CB was chosen as a substrate or as a catalyst for CNT growth because it has been reported to give high catalytic activity for the decomposition of hydrocarbons with a high production yield of hydrogen.[11-14] Moreover, CB is a well-developed carbonaceous material with wide applications in rubber reinforcement, pigment-based inks, black matrix resistance in thin-film transistor displays, anodes in lithium-ion batteries and catalyst support in fuel cells. Additionally, few studies revealed that a physical mixing of CNT and CB can significantly improve their performances in energy storage devices[15] and rubber reinforcement.[16] Jang et al. used a physical mixture of carbonaceous materials, i.e., graphene, CNTs and CB, as the anode of a lithium-ion battery, achieving a high electronic capacity and high power density compared with the conventional anode component (graphite and CB).[15] Moreover, the recharge time of this newly developed lithium-ion battery was considerably shortened to the scale of minutes, potentially leading to a remarkable improvement in next-generation lithium-ion batteries. Li et al. reported that multi-walled CNTs could improve the reinforcement and electronic conductivity of copolymer in comparison with normal CB systems.[16] Thus, the integrated CNTs/CB hybrid structures can be applied in well-defined systems without considering the dispersion problem caused by CNTs or with only a slight adjustment required to the dispersion conditions. These studies demonstrate that a bi-functional structure of CNT/CB should exhibit superior electronic conductivity and polymer reinforcement compared with a physical mixture of CNT and CB.

Although, we have demonstrated that the growth of CNTs on typical carbonaceous materials, such as porous carbon and defect-containing graphite, without metal catalysts is a promising route. However, achieving a

control over the resulting hybrid structures remains a challenge. This paper demonstrates a one-step preparation of CNTs/CB and CNFs/CB hybrid structures, an approach that has not been previously discussed. CNTs/CB or CNFs/CB hybrid structures through a metal-free process and also provides new concepts for manufacturing CB in an industrial scale.

Experimental

Materials. A series of CBs (N110, N220, N330, N339, N550, N774 and BP2000) were used as the catalysts to grow CNTs by MCF-CVD at various temperatures (700-1000 ^{o}C). The physical properties of these CBs are displayed in Table 1. N110, N220, N330, N339, N550 and N774 are usually used in rubber reinforcements for tire applications. All of the CBs were supplied by the China Synthesis Rubber Corporation in Taiwan. BP2000 was purchased from Cabot Co., USA.

Purification of Carbon Black. In order to eliminate the influence of residual contaminating metals during the manufacture of the CB samples, they were treated in 1 M hydrochloric acid for 48 h, washed in pure water to remove the acid solution, and then dried in an oven at 120 ^{o}C before use. After the acid treatment, the original trace amounts (ppm level, shown in Table 1) of metallic impurities, such as Ni and Fe (Co and other highly active catalysts for CNT growth were not detected) for all untreated CB samples were reduced to be undetectable measured by induced coupled plasma mass spectrometry (ICP-MS) (PE-SCIEX ELAN 6100 DRC).

Carbon Nanotube Growth. Typical experiments were performed in a horizontal quartz tube, 30 mm in diameter and 1000 mm in length using a single-stage furnace. Various CBs were used as the catalysts with gaseous (ethylene and acetylene) and liquid (cyclohexane and ethanol) carbon-bearing molecules as the carbon sources for CNT growth. The weight of CB was approximately 100 mg. Ethylene or acetylene was diluted with argon (C_2H_4/Ar=1/9 or C_2H_2/Ar=1/9) at a flow rate of 100 mL/min under atmospheric pressure. For the liquid carbon source, cyclohexane or ethanol, which was put in a liquid tank and introduced to the CVD reactor by a vacuum pump through a needle valve to control the pressure at 76 mmHg (1/10 atm) similar to the proportion of gaseous carbon sources at atmospheric pressure during the CNT growth process. The CNT growth period was fixed at 30 min in the temperature range of 750-1000 ^{o}C. We also performed the in-situ metal-free CVD experiments with diluted ethylene and acetylene in a thermogravimetric analysis (TGA, TA-Q500 and Perkin Elmer-7A) chamber, where it is easy to monitor the growth yield from the cracking of various carbon sources, as well as to examine the proportion of CNTs and amorphous carbons by slow oxidation.[9, 10] TGA measurements were conducted on samples weighting approximately 10 mg.

Materials Characterization. The CNT growth yields on various CB samples were conducted by TGA. A scanning electron microscope (SEM, JEOL JSM-6700F) and transmission electron microscope (TEM, JEOL AEM-3010 and JEM 2100) equipped with an energy dispersive spectrometer (EDS) were used to investigate the micro- and nano-scale structural morphologies of the as-grown samples and perform elemental analyses. Raman scattering spectroscopy (JOBIN-YVON T64000) was performed with a laser excitation wavelength of 532 nm.

Table 1. Physical properties of carbon black.

Carbon Black	Total surface Area/external surface area (m^2/g)[a]	Particle size (nm)[b]	Metal impurity before/after acid treatment (ppm)[c]
N110	140/126	19	14.9/bdl[d]
N220	118/112	20	13.8/bdl
N330	80/79	26	15.7/bdl
N339	92/90	24	17.5/bdl
N550	40/40	43	23.4/bdl
N774	28/28	60	25.4/bdl
BP2000	1475/875	12	13.7/bdl

[a] Measured by nitrogen adsorption based on the Brunauer-Emmet-Teller method (ASTM D4820-99). External surface area means total surface area subtract micro-pore surface area.
[b] Estimated by TEM measurements for approximately 100 particles.
[c] The content of the iron-group (Fe, Co and Ni) metal impurities in nitric acid treated samples measured by ICP-MS.
[d] Note: bdl = below detection limits.

Results and discussion

Usually, the choice of carbon sources was not considered as a decisive factor for CNT growth using metal-assisted CVD owing to similar active positions of metal nanoparticles. However, CNT growth using MCF-CVD would severely concern the kind of carbon sources and were discussed less. In our previous studies, we observed that ethylene was an active carbon source for CNT growth using MCF-CVD.[9, 10] However, the pathway for ethylene during the formation of CNTs is still unclear. Additionally, it is worth to understand that whether other well-known carbon sources, e.g. acetylene, ethanol and cyclohexane, used in the high-yield synthesis of CNTs through metal-assisted CVD could perform the similar results with that of ethylene. Therefore, a comparable study of various carbon sources yielding the as-expected CNTs using MCF-CVD is the first goal of this study. Referring to the recent review articles, Ahmed et al.[17] and Shaikjee et al.[18] described the role of the hydrocarbon source on the growth of carbon materials via metal-assisted or metal-free processes. Notably, the selection of hydrocarbon sources in the metal-assisted process has a relatively minor effect on the growth of CNTs/CNFs, especially for the iron-group metal catalysts. The main process of the metal-assisted growth of CNTs consists of first the decomposition of hydrocarbons and then the formation of CNTs through bulk diffusion (iron-group metal catalysts) or surface diffusion (non-iron group metal catalysts, e.g., copper, silver and gold)[19, 20] of the deposited carbon species. However, in the MCF-CVD process, the selection of the carbon source should be the key factor in the growth of CNTs/CNFs due to a lack of assistance from metal nanoparticles. Previous studies by Liu et al revealed that alcohol-based hydrocarbons are suitable for the growth of single-walled CNTs over SiO_2-based catalysts.[5, 6] Methane,[7] ethanol[8] and ethylene[9, 10] are also available as carbon sources for the growth of CNTs on nano-diamond or defect-rich carbon. However, thermal decomposition of

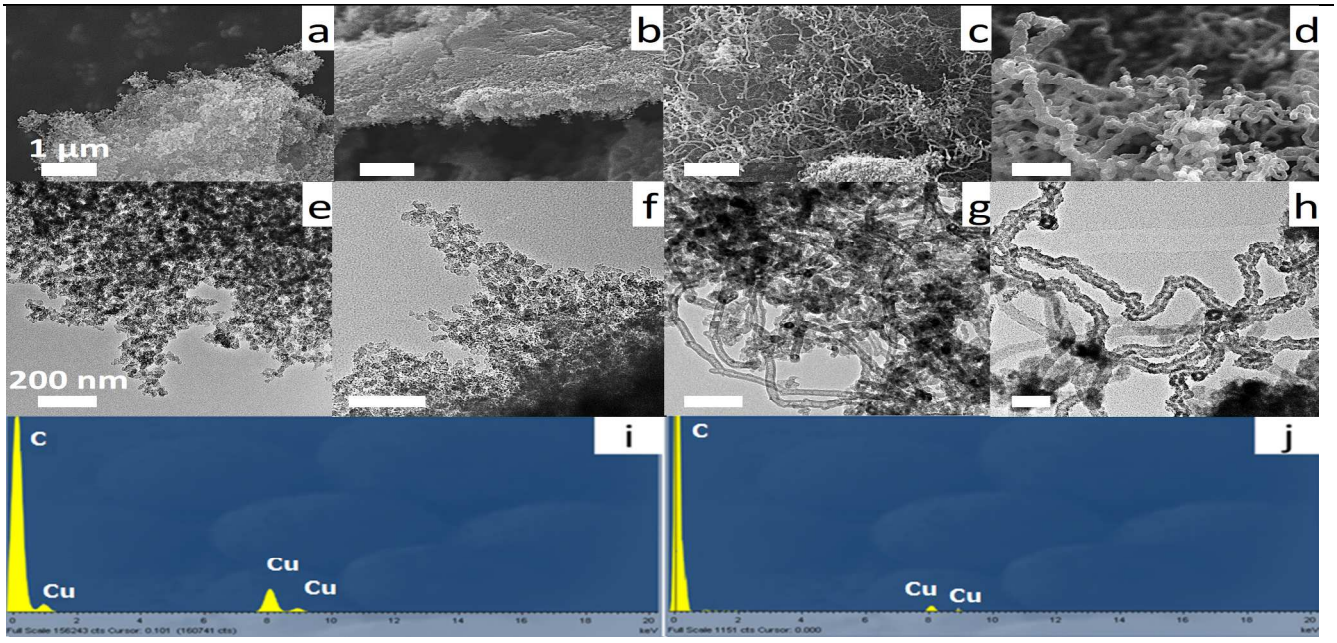

Figure 1. SEM images of carbon nanostructures grown on carbon black-BP2000 with different carbon feedstock: a) cyclohexane, b) ethanol, c) ethylene and d) acetylene. e-h) are TEM images of a-d) respectively. i) and j) are EDS spectra of c) and d) respectively. The growth temperature is at 850 °C with various carbon sources for 30 min. The scale bar in a)~d) is 1 µm and the scale bar in e)~h) is 200 nm.

methane or other hydrocarbons on elemental carbon catalysts during 800-900 °C only produced amorphous carbon (a-C) instead of CNTs or CNFs, as reported by Muradov et al.[12] Therefore, more studies are required on the growth of CNTs or CNFs using carbon catalysts with various carbon sources.

Figure 1 presents SEM (a-d) and TEM (e-h) micrographs of the as-grown carbon structures on a CB (BP2000, 1475 m^2/g) surface by thermal CVD of cyclohexane, ethanol, ethylene and acetylene at 850 °C without any metal catalysts. The EDS spectra shown in Figure 1i and 1j confirm that the as-grown CNTs in Figure 1c and 1d were not influenced by unwanted metal catalysts. Actually, we conducted the EDS measurements more than 20 times on different positions of CB-BP2000, only copper and carbon signals were observed. The copper signal should arise from the TEM copper grid and sample holder. This also indicates that HNO_3 pre-treated CB can lower down the metal residuals to a negligible influence on the growth of CNTs.

Figure 1 depicts that ethylene and acetylene are active carbon sources for CNT growth; however, no CNTs were observed when the carbon feedstock was replaced with ethanol or cyclohexane. It has been known for over 20 years that CVD of our selected hydrocarbons on reactive metal catalysts can produce CNTs or CNFs. Without the assistance of metal catalysts, the decomposition of hydrocarbons was guided by typical chemical structures, e.g. SiO_x,[7] meta-stable carbon layers,[8] or defect-rich positions,[10] on non-metal catalysts. For carbon catalysts, several reports have pointed out that non-crystalline carbons such as carbon black or activated carbon can serve as the elemental catalyst to crack the hydrocarbons into carbon species and hydrogen. Muradov et al. revealed that the deposited carbon species can generate remarkable activity for the decomposition of hydrocarbons over several hours.[11] Szymanski et al. reported that ethanol partially decomposes to CH_3- and CH_3COH- species on carbon surfaces and then forms ethylene or aldehyde via a surface chemical reaction at low temperatures (50-320 °C).[21] Gong et al. presented the thermal decomposition of cyclohexane through a theoretical kinetic study, which determined that the main products are 1,3-butadiene, ethylene, propylene and 1-hexene.[22] In these studies, ethylene is one of the gaseous products during the catalytic decomposition of ethanol on carbon or thermal cracking of cyclohexane. Accordingly, in our study, we expected that cyclohexane and ethanol are active carbon sources for the growth of CNTs or CNFs instead of a-C. However, we only observed a-C generated on CB with CVD of cyclohexane and ethanol. This implies that thermal decompositions of ethanol and cyclohexane on CB mainly proceed with different pathways towards the formation of carbon species, which led to the formation of a-C instead of CNTs. In other words, even ethylene is a product of decomposition of ethanol and cyclohexane, the further re-adsorption of ethylene and decomposition into the nuclei for the formation of CNTs did not happen. This also indicates that the formation of the as-grown CNTs using the CB catalyst is guided by the catalytic decomposition of carbon-bearing species not resulting from a thermal pyrolysis process.[23]

A further examination of gas-phase components during the MCF-CVD process is required to understand the decomposed pathways of various carbon-bearing molecules on CB. The results are shown in **Table 2**. Interestingly, the yielded hydrogen contents for using ethylene and acetylene as carbon sources are higher than

those resulting from the catalytic decomposition of cyclohexane and ethanol. Although methane and ethylene are mainly products of ethanol using catalytic pyrolysis on CB, however these well-known carbon sources were not further decomposing into active carbon components for growing CNTs. Similar results (mainly C_2~C_4 related products) were observed when using cyclohexane as the carbon feedstock. This hints that the real formation of CNTs should follow a further decomposition of adsorbed C_2 species on CB surface through a strong gas-substrate interaction. On the contrary, the C_2 species generated from ethanol or cyclohexane would give a weak-interaction on CB surface and further yielded gaseous hydrocarbons through a surface or gas-phase radical collision subsequently.

Table 2 Comparison of the carbon distribution in gaseous hydrocarbons[a] and solid carbon generated over CB-BP2000 using chemical vapour deposition with various carbon sources after 60 min at 850 ^{o}C

Carbon sources	H_2 (%)	CH_4 (%)	C_2[c] (%)	C_3+C_4 (%)	carbon (%)	others (%)
Ethylene	**40.8**	**5.0**	**31.1**	**1.3**	**20.9**	**0.9**
Acetylene	**43.4**	**6.7**	**17.1**	**3.1**	**27.2**	**2.5**
Cyclohexane	**17.2**	**5.1**	**34.9**	**31.6**	**11.0**	**0.2**
Ethanol	**24.6**	**21.0**	**39.3**	**bdl**[b]	**4.5**	**10.6**

[a]Gaseous hydrocarbons were collected and analysed by gas chromatography (Shimadzu GC-2014) using a 6-ft Porapack Q 80/100 mesh column with a flame ionization detector. Gaseous samples were collected just after CNT growth termination and sealed with stainless steel ball valves. He was quantified as the carrier gas.

[b] Note: bdl = below detection limits.

[c] C_2 species include C_2H_2, C_2H_4 and C_2H_6.

Next, close-up views of the as-grown CNTs produced by thermal CVD of ethylene and acetylene were obtained by TEM and are displayed in Figure 2a and 2b, respectively. Apparently, the CNTs grown from the ethylene decomposition adopt a bamboo-like structure, while turbostratic CNFs (T-CNFs) are formed by the decomposition of acetylene. In Figure 2c and 2d, the diameter-distribution histograms of the as-grown CNTs and CNFs shown a range of 40-80 nm (approximately 76%) and 80-120 nm (approximately 68%), respectively.

The growth yield of CNFs was conducted in a TGA chamber with a weigh-gain for thermal decomposition of ethylene or acetylene at 850 ^{o}C for 30 min, or an oxidation of the as-grown CNTs by TGA according to previous studies.[9, 10] The growth yields of as-grown bamboo-like CNTs (BL-CNTs) and T-CNFs are 1.71 g CNT soot/g CB·h and 2.43 g CNF soot/g CB·h, respectively. The distinct growth features of carbon nanostructures (BL-CNT and T-CNFs) on CB with different carbon feedstock demonstrate the diverse diffusion rates of the deposited carbon species. If the diffusion rate of the carbon species is higher than that of the graphitic alignment, then the turbostratic structure will form; otherwise, the CNT-like structure will dominate.

The as-grown carbon materials with various carbon sources exhibit different pathways from the decomposition of hydrocarbon to the formation of carbon nano-structures (CNT, CNF or a-C). Although the explicit mechanism for this finding is unclear, however, few reports have proved that ethylene and acetylene would proceed through elementary decomposition on CB at defect-rich positions to generate carbon species and then form CNTs or CNFs, respectively, through self-assembly on the CB surface.[9, 10] This self-assembling behaviour of CNTs and CNFs is similar to the surface-diffusion model for metal-assisted routes reported by Robertson et al.[24, 25] (iron-based metal catalysts), Tagaki et al.[19, 20] (non-iron metal catalysts) and Lin et al.[9, 10] (non-metal substrates). For metal-assisted process, the surface-diffusion model clearly states that the outer-diameter and structural features (SWCNT, MWCNT or a-C) of the as-grown CNTs are guided by the size of the metal clusters. Normally, small metal clusters (1-5 nm) will generate SWCNTs, while MWCNTs will be the main product when the clusters are between 5-20 nm. Larger metal clusters (> 50 nm) would generate graphitic–like carbon or a-C. For non-metal substrates, previous studies described a self-assembling formation of MWCNTs on defect-rich carbon or graphite surface via active nucleation sites - nanobumps.[10]

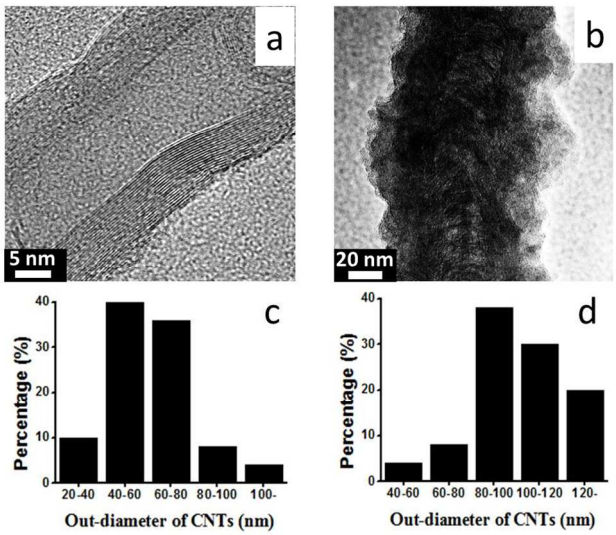

Figure 2. HR-TEM images of the as-grown carbon nanostructures on carbon black-BP2000 with different carbon sources: a) ethylene and b) acetylene. The outer-diameter distribution histograms of the as-grown CNTs and CNFs from a) and b) are shown in c) and d), respectively. The growth temperature is at 850 ^{o}C with carbon sources for 30 min.

Determining the activation energy for CNT growth over CB catalyst will assist in understanding the growth mechanism. Therefore, understanding the kinetics of CNT growth over CB catalyst from 750 to 1000 ^{o}C will be helpful to determine the diffusion pathway of deposited carbon species on CB surface and the route of fabrication into CNTs. We propose that CNT growth over CB catalyst occurs together with dissociative adsorption of ethylene on the CB surface and a rate-determining step of

carbon species diffusion, which are governed by different activation energies. Generally, the formation of CNTs by the metal-free route follows the self-assembling model with a lower activation energy (<1 eV), while the metal catalyst overcomes the penetration route of carbon diffusion through metallic nanoparticles with a high activation energy (> 1 eV, even as high as 2.5 eV).

It is interesting that only a-C can form on CB when cyclohexane and ethanol are used as the carbon feedstock. Li et al. reported a stepwise decomposition pathway (an eight-step procedure) of ethanol to elemental carbons on well-defined Pd (111) surface.[26] As we know, the amorphous structures of CB consist of randomly defect-rich positions, which will not provide continuous active sites for the decomposition of ethanol or cyclohexane to become carbon species for CNT growth. Accordingly, a-C is the main product obtained when using cyclohexane or ethanol as the carbon source.

In Figure 1 and 2, we know that ethylene is the better candidate as carbon source for CNT growth. To understand the growth mechanism of CNTs on CB using metal-free CVD with ethylene as the carbon source, we conducted the CVD process at different temperatures (750-1000 ^{o}C). Here, we did not observe any CNTs while the reaction temperatures were below 800 ^{o}C. The SEM micrographs are shown in the left panel of Figure 3. Table 4 presents the growth yields and graphitic features of the as-grown CNTs at different temperatures. In the right panel of Figure 3, an Arrhenius plot of ln (growth yield) vs. 1/T (K) yields the activation energy of the CNT growth to be 59.0 kJ mol^{-1} (~0.61 eV), which is close to surface diffusion energy of carbon on metal or non-metal surface.[24, 25]

In the classical model of CNT growth, the ethylene adsorbs on the catalyst surface and dissociates into carbon atoms and hydrogen (eqn. 1). In Table 2, the gas analyses shows that the strong interaction of C_2 species with CB would dominate the CNT formation. There are several possible elementary reaction routes for the CNT formation. One possibility was proposed by C. T. Wirth et al.[25] through a kinetic study of CNT formation with a surface diffusion model. In this study, the CNT formation on CB surface should follow their model as below.

$$C_2H_{4\ gas} \leftrightarrows C_2H_{4\ ads}$$
$$C_2H_{4\ ads} \leftrightarrows 2C_{ads} + 2H_2 \quad (1)$$

We propose that this reaction consists of two rate constants for forward and backward reactions (eqn. 2 and 3)

$$R_1 = k_1 [C_2H_4] \quad (2)$$
$$R_{-1} = k_{-1} [C_{ads}]^2[H_2]^2 \quad (3)$$

These reactions are followed by the slower process of carbon diffusion over the CB surface and assembly to form CNTs (eqn. 4).

$$C_{ads} \rightarrow C_{CNT} \quad (4)$$

which is determined by the growth rate.

The growth rate of this study is expressed according to the Arrhenius equation as follows:

$$R_{CNT} = k_2 [C_{ads}] \quad (5)$$

If $k_{-1} >> k_2$ (because the CNT formation is usually a rate-determining step of reaction), then this equivalent to a pre-equilibrium of dissociate carbon atoms regulated by an equilibrium constant k (eqn. 6)

$$k = k_1/k_{-1} = [C_{ads}]^2[H_2]^2/[C_2H_4] \quad (6)$$

The overall CNT growth rate is proportional to $[C_{ads}]$ concentration or to the $[C_2H_4]$ concentration to the power of 0.5 (eqn. 7)

$$R_{CNT} = k_2 [C_{ads}] \sim k_2(k_1/k_{-1})^{0.5}[H_2]^{-1} [C_2H_4]^{0.5} \quad (7)$$

According to the Arrhenius plot ln k = ln A-ΔE/RT (k is a reaction constant, ΔE is the activation energy of the reaction), one can obtain the activation energy of the formation of CNTs, which is an index to indicate the formation of CNTs is through bulk-diffusion or surface-diffusion on catalysts. Here, the growth yields (R_{CNT}) of the as-grown CNTs under atmospheric pressure for different growing temperatures at 750-1000 ^{o}C were determined by TGA based on the reported method. The data are displayed in Table 3. Because the growth of CNTs on CB catalyst does not occur in the form of dense mats, it is more appropriate to present the growth yield (g CNT soot/g C h^{-1}) instead of the growth rate (mm CNT h^{-1}). Plotting ln R vs. 1/T demonstrates a linear dependence as shown in the right panel of **Figure 3**.

Table 3. The growth yields and diameter distributions as well as the I_G/I_D ratios of the as-grown CNTs at various temperatures on CB-BP2000 under 10% C_2H_4/Ar at a flow rate of 100 mL/min for 30 min.

Temperature (^{o}C)	CNT growth yield (g CNT soot/g CB·h)	I_G/I_D ratio	CNT diameter distribution (nm)
800	1.20	0.72	20-60
850	1.71	1.10	20-80
900	2.13	1.01	20-120
950	3.01	0.86	40-150
1000	3.20	0.70	> 200 nm

The activation energy is found to be 59.0 kJ mol^{-1}, which is much smaller than that was estimated from iron-based catalysts.[24, 25] This demonstrates that CB catalysts have remarkable ethylene cracking activity at growth temperatures (800-1000 ^{o}C) and that the deposited carbon species will only diffuse on the surface of CB according to the vapour-solid-surface-solid (VSSS) model.

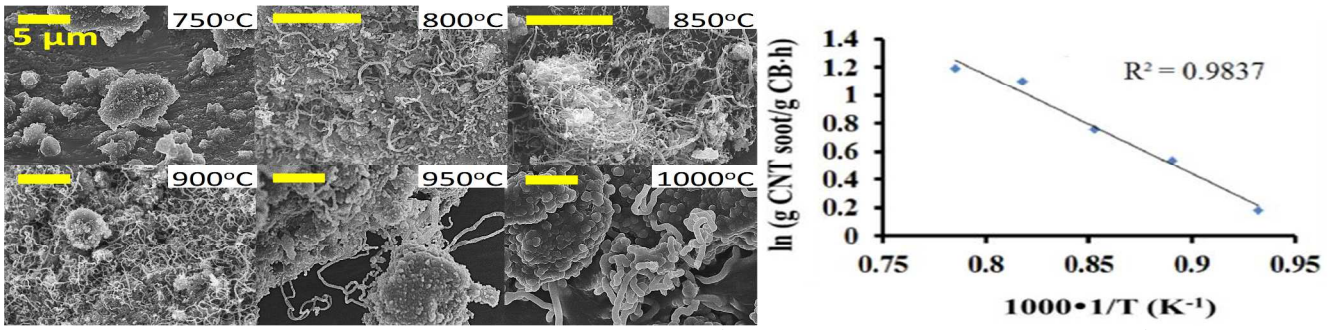

Figure 3. Left panel: SEM micrographs of the as-grown a-C (750 °C) and the as-grown CNTs (800-1000 °C). Right panel: Arrhenius plot for the growth rate of CNTs, providing the activation energy, ΔE = 59.0 kJ/mol.

Figure 4 displays the Raman spectra and I_G/I_D ratios of the hybrid CNT/CB samples fabricated at various temperatures. CNT growth at 850 °C clearly leads to a higher yield and a higher I_G/I_D ratio. A clear blue-shift at D band of the hybrid CNT/CB sample was also observed at growth temperature of 850 °C, which is not caused by the structural change of CB at various temperatures. This indicates that the CNTs generated at 850 °C displaying better graphitic structures or less intertube-interaction of the as-grown CNTs.[26]

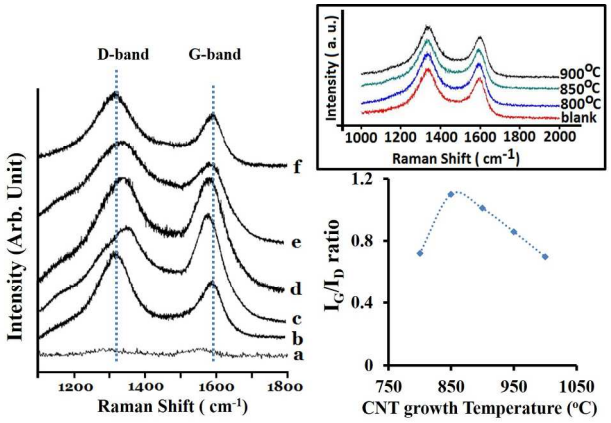

Figure 4. Left panel: Raman spectra of the samples following CNT growth at various temperatures: a) original CB-BP200, b) 800 °C, c) 850, d) 900, e) 950 and f) 1000 °C. Right panel: the I_G/I_D ratios of as-grown CNT versus growth temperature. The insert shows the Raman spectra of CB treated at different temperatures in Ar for 30 min.

Up to now, we have described the growth of CNTs on CB with ethylene and acetylene should proceed with a surface-diffusion model. However, two main issues need to be clarified to understand the metal-free growth mechanism of CNTs on CB. These include (1) the locations of the active sites on CB for promoting CNT growth and (2) whether this mechanism is only applicable for the porous carbon black-BP2000. To understand CNT growth catalysed by CBs, we carefully examined the original surface structure of CB and the root positions of the as-grown CNTs on the CB surface by TEM measurements via a short growth period (1-5 min). Figure 5 presents the TEM micrographs of the as-grown CNT generated on a CB particle with different growth times. Figures 5a and 5c depict the CNT growth status for 1 min and 5 min, respectively, and zoomed-in images for the two time periods are displayed in Figures 5b and 5d. Apparently, the newly grown CNT is likely extruded from a CB particle as shown in Figure 5b.

At longer growth times (5 min), a tubular structure through a CB particle is observed without the assistance of metal elements. This indicates that the deposited carbon species will assemble a multi-layer graphene-like structure and extrude (or lift-off) to be MWCNTs on CB particles (see Figure 5b). This reveals a direct evidence for CNT growth on a non-metal substrate. Unlike the growth behaviours of CNTs on semi-conductive nanoparticles, which described the chemical compositions dominating the CNT growth. Here, CB nanoparticles present spherical structures with pure carbon atoms as the CNT caps to grow MWCNTs. This nanoparticle-assisted growth model obeys the VSSS mechanism.

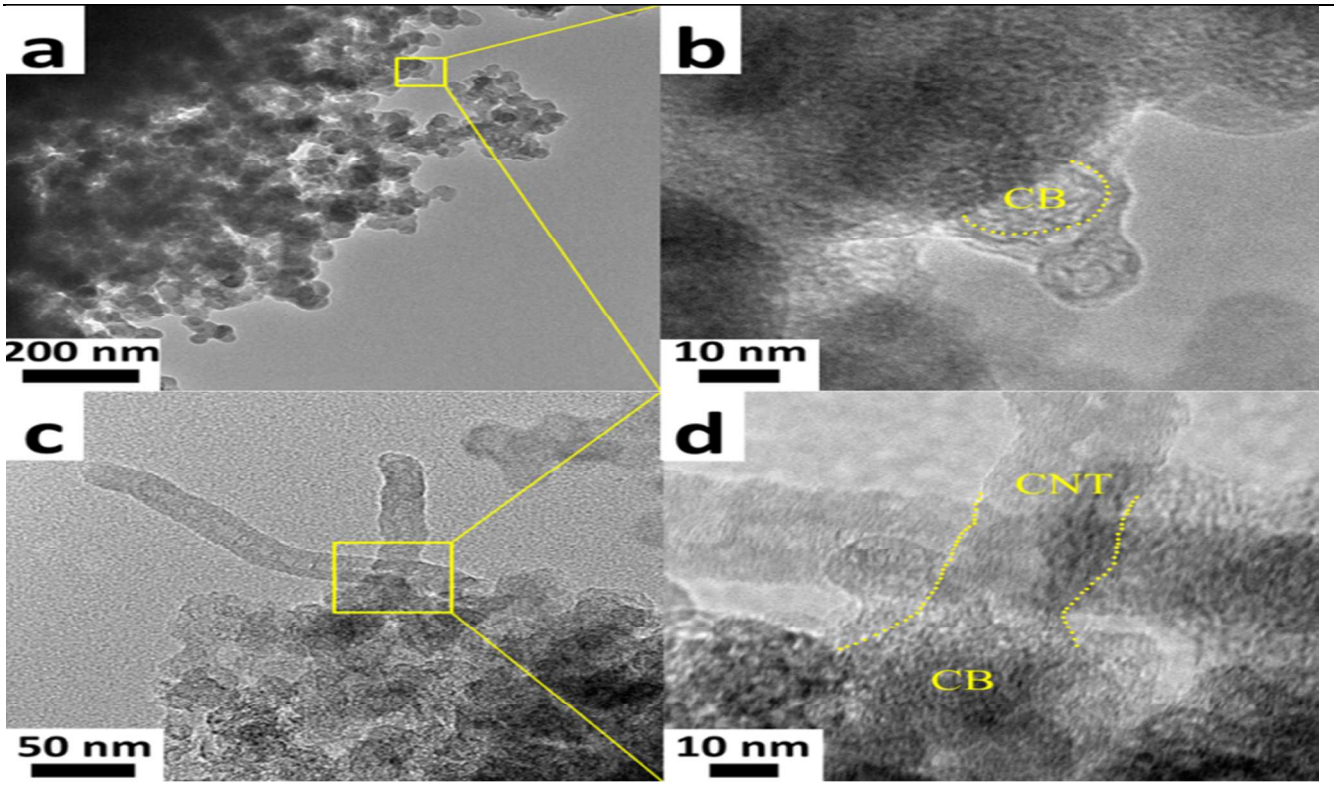

Figure 5. TEM micrographs of CNTs grown on CB-BP2000 for a) 1 min and c) 5 min. b) and d): Close-up images of a) and c), respectively. The growth temperature is at 850 °C with diluted ethylene (Ar/C_2H_4=9/1=100 mL/min) at different times.

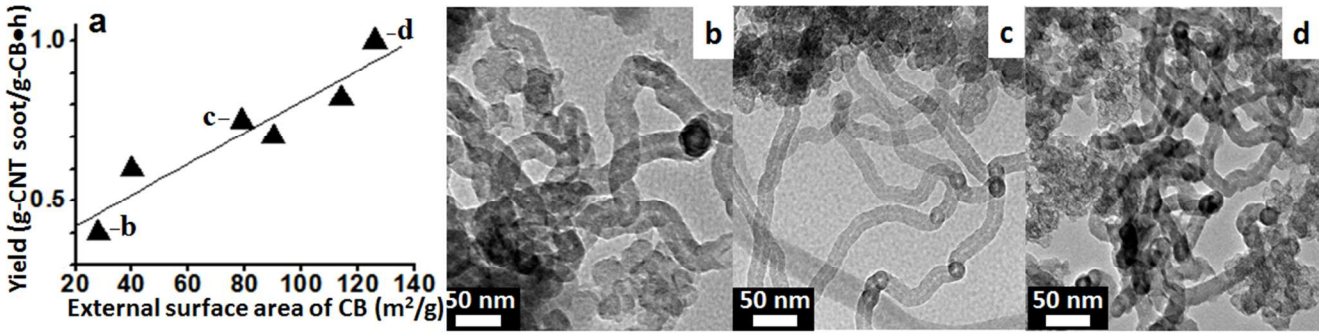

Figure 6. a) A plot of the growth yields of the as-grown CNT soot versus the specific surface area of the CB. b) ~ d): TEM images from three different points in plot a). The growth temperature is at 850 °C with diluted ethylene (Ar/C_2H_4=9/1=100 mL/min) at different times.

Our previous studies demonstrated that the pore structure and defect-rich positions are the key factors promoting the growth of CNTs.[9, 10] The quantitative description of the pore structure and defect-rich positions for a typical material are generally estimated by the BET surface area measurement. Thus, if our understanding is correct, the CNT growth yields will exhibit a linear correspondence with the BET external surface areas of various kinds of CB. Therefore, we used a series of CB (physical properties shown in Table 1) with different BET external surface areas to conduct ethylene CVD with the same conditions as the CB-BP2000. The CNT growth yield exhibits a linear relationship with the BET surface area of CBs as shown in ~~the left panel of~~ Figure 6a. The ~~right panel of~~ Figure 6b-d presents TEM micrographs of the as-grown CNTs using selected CB samples. This suggests that the growth of CNTs was catalysed by high-surface-energy sites on the CB surface. The high-surface-energy sites include defect-rich or unsaturated carbon structures that acted as catalysts to first decompose gaseous hydrocarbon feedstock and then promote the formation of CNTs through a self-assembly process. The surface features of CB act like a capping structure for CNT growth. In addition, the outer-diameters of the as-grown CNTs on varying CBs are normally above 20 nm, similar to the average particle size of the CBs shown in Table 1. These data reveal that the active sites for CNT growth on CB catalysts correspond with defect-rich positions and spherical CB nanoparticles, with the former promoting the decomposition of hydrocarbons and the latter

representing the CNT growth site. Therefore, the most likely mechanism for CNT growth on CB by the metal-free route is hydrocarbon decomposition into carbon species at high-energy positions (porous structures or defect-rich sites) followed by diffusion and then assembly of carbon species on the cap-like surface of CB to form CNTs. This also provides a reasonable explanation for the lack of any SWCNTs or short-diameter (< 10 nm) MWCNTs.

Conclusions

Here, we report a simple method to develop a hybrid carbon structure-CNT/CB and CNF/CB using a metal-free route at a mild temperature. This approach enables the development of a unique C/C composite through a one-step method without the interference of unwanted metal nanoparticles. The CNT growth behaviour clearly follows a vapour-solid-surface-solid model through surface-diffusion over CB nanoparticles. These findings may facilitate a new approach to the synthesis of CNTs or CNFs using metal-free methods.

Acknowledgements

J. H. Lin expresses his sincere appreciation to the National Science Council of the Republic of China for financially supporting this study (NSC-101-2113-M-024-002).

Notes and references

Dept. of Materials Science, National University of Tainan, 33, Sec. 2, Shu-Lin St., Tainan70005, Taiwan. E-mail: janusjhlin@mail.nutn.edu.tw

1. P. Liu, Eur. *Polym. J.* 2005, **41**, 2693.
2. B. I. Kharisov, O. V. Kharissova, H. L. Gutierrez and U. O. Méndez, *Ind. Eng. Chem. Res.* 2009, **48**, 572.
3. N. Ning, S. Fu, W. Zhang, F. Chen, K. Wang, H. Deng, Q. Zhang and Q. Fu, *Prog. Polym. Sci.* 2012, **37**, 1425.
4. F. Mammeri, J. Teyssandier, C. Connan, E. Le Bourhis and M. M. Chehimi, *RSC Adv.* 2012, **6**, 2462.
5. B. Liu, W. Ren, L. Gao, S. Li, S. Pei, C. Liu, C. B. Jiang and H. M. Cheng, *J. Am. Chem. Soc.* 2009, **131**, 2082.
6. S. Huang, Q. Cai, J. Chen, Y. Qian and L. Zhang, *J. Am. Chem. Soc.* 2009, **131**, 2094.
7. B. Liu, D. M. Tan, C. H. Sun, C. H. Liu, C. Liu, W. C. Ren, F. Li, W. J. Yu, L. C. Yin, L. L. Zhang, C. B. Jiang and H. M. Cheng, *J. Am. Chem. Soc.* 2011, **133**, 197.
8. D. Takagi, Y. Kobayashi and Y, Homma, *J. Am. Chem. Soc.* 2009, **131**, 6922.
9. J. H. Lin, C. S. Chen, H. L. Ma, C. W. Chang, C. Y. Hsu and H. W. Chen, *Carbon* 2008, **46**, 1619.
10. J. H. Lin, C. S. Chen, M. H. Rümmeli, A. Bachmatiuk, Z. Y. Zheng, H. L. Ma, B. Büchner and H. W. Chen, *Chem. Mater.* 2011, **23**, 1637.
11. N. Muradov, F. Smith and A. T. Raissi, *Catal. Today* 2005, **102-103**, 225.
12. N. Muradov, P. Choi, F. Smith and G. Bokeman, *J. Power Sources* 2010, **195**, 1112.
13. J. Zhang, D. S. Su, A. Zhang, D. Wang, R. Schlögl and C. Hébert, *Angew. Chem. Int. Ed.* 2007, **46**, 7319.
14. J. Zhang, X. Liu, R. Blume, A. Zhang, R. Schlögl and D. S. Su, *Science* 2008, **322**, 73.
15. B. Z. Jang, C. Liu, D. Neff, Z. Yu, M. C. Wang, W. Xiong and A. Zhamu, *Nano Lett.* 2011, **11**, 3785.
16. Y. Li and H. Shimizu, *Macromolecules* 2009, **42**, 2587.
17. S. Ahmed, A. Aitani, F. Rahman, A. Al-Dawood and F. Al-Muhaish, *Appl. Catal. A: General* 2009, **359**, 1.
18. A. Shaikjee and N. J. Coville, *Carbon* 2012, **50**, 3376.
19. D. Takagi, Y. Homma, H. Hibino, S. Suzuki and Y. Kobayashi, *Nano Lett.* 2006, **6**, 2644.
20. D. Takagi, Y. Kobayashi, H. Hibino, S. Suzuki and Y. Homma, *Nano Lett.* 2008, **8**, 832.
21. G. S. Szymański, G. Rychlicki and A. P. Terzyk, *Carbon* 1994, **32**, 265.
22. C. M. Gong, Z. R. Li and X. Y. Li, *Energy Fuels* 2012, **26**, 2811.
23. R. Xiang, E. Einarsson, P. Zhao, S. Harish, K. Morimoto, Y. Miyauchi, S. Chiashi, Z. Tang and S. Maruyama, ACS Nano 2013, **7**, 3095.
24. S. Hofmann, R. Sharma, C. Ducati, G. Du, C. Mattevi, C. Cepek, M. Cantoro, S. Pisana, A. Parvez, F. Cervantes-Sodi, A. C. Ferrari, R. Dunin-Borkowski, S. Lizzit, L. Petaccia, A. Goldoni and J. Robertson, *Nano Lett.*2007, **7**, 602.
25. C. T. Wirth, C. Zhang, G. Zhong, S. Hofmann and J. Robertson, *ACS Nano* 2009, **3**, 3560.
26. M. Li, W. Guo, R. Jiang, L. Zhao and H. Shan, *Langmuir* 2010, **26**, 1879.
27. L. Bokobza and J. Zhang, *Express Polym. Lett.* 2012, **6**, 601.